

Spherical Nucleic Acids for Topical Treatment of Hyperpigmentation

Yang Fang, Xueguang Lu, Dali Wang, Jiansong Cai, Yuyan Wang, Peiru Chen, Mengqi Ren, Hao Lu, Jennifer Union, Lei Zhang, Yehui Sun, Fei Jia, Xi Kang, Xuyu Tan, and Ke Zhang*



Cite This: *J. Am. Chem. Soc.* 2021, 143, 1296–1300



Read Online

ACCESS |



Metrics & More



Article Recommendations



Supporting Information

ABSTRACT: Oligonucleotide-based materials such as spherical nucleic acid (SNA) have been reported to exhibit improved penetration through the epidermis and the dermis of the skin upon topical application. Herein, we report a self-assembled, skin-depigmenting SNA structure, which is based upon a bifunctional oligonucleotide amphiphile containing an antisense oligonucleotide and a tyrosinase inhibitor prodrug. The two components work synergistically to increase oligonucleotide cellular uptake, enhance drug solubility, and promote skin penetration. The particles were shown to reduce melanin content in B16F10 melanoma cells and exhibited a potent antimelanogenic effect in an ultraviolet B-induced hyperpigmentation mouse model.

Hyperpigmentation, a common condition associated with exposure to ultraviolet (UV) light or skin inflammation, occurs when excess melanin forms deposits in the skin.¹ Melanogenesis takes place in melanocytes, which are located at the basal layer of the epidermis.² It is mainly regulated by tyrosinase (TYR) and other tyrosinase-related proteins (TRPs).^{3,4} These enzymes are transcriptionally regulated by the microphthalmia-associated transcription factor (MITF).⁵ Melanin biosynthesis can be stimulated with the increased production of MITF, which is a result of melanocortin 1 receptor (MC1R) binding to the α -melanocyte-stimulating hormones (α -MSHs).^{6–8} Current treatments for hyperpigmentation include physical means such as laser/chemical skin resurfacing and microdermabrasion, which need to be carefully managed to minimize skin damage,⁹ and transdermal delivery of TYR inhibitors. The latter is a less invasive and more convenient alternative that does not interfere with the patient's normal daily life.

Commonly used TYR inhibitors include kojic acid, phenylethyl resorcinol, and hydroquinone, which perform well *in vitro* but suffer from side-effects such as skin irritation and/or limited absorption.^{10,11} Phenylethyl resorcinol (PR), a particularly potent TYR inhibitor,¹² which inhibits mushroom tyrosinase ~22 times more effectively than kojic acid,¹³ has been adopted as the active ingredient in depigmenting commercial products.¹⁴ However, the poor aqueous solubility of PR reduces skin absorption and overall efficacy.¹⁴ Attempts to target upstream proteins using anti-MITF or anti-MC1R siRNA together with a transdermal peptide have been shown to deplete target transcripts and produce a skin-lightening effect on patients with hyperpigmented facial lesions after 12 weeks of topical treatment.¹⁵ However, efficient topical delivery of oligonucleotide drugs across intact skin remains a lasting challenge due to the stratum corneum,¹⁶ which is a strong barrier of the epidermis that impedes a wide range of agents intended for the skin.^{17–19} Recently, spherical nucleic acids (SNAs), which are core–shell nanoparticles with a densely functionalized oligonucleotide shell and a rigid core

(metallic or nonmetallic particles), have been shown to penetrate the skin barrier and abolish target gene expression in the epidermis and dermis with only 3 weeks of topical treatment in the absence of a transfection agent.^{20,21}

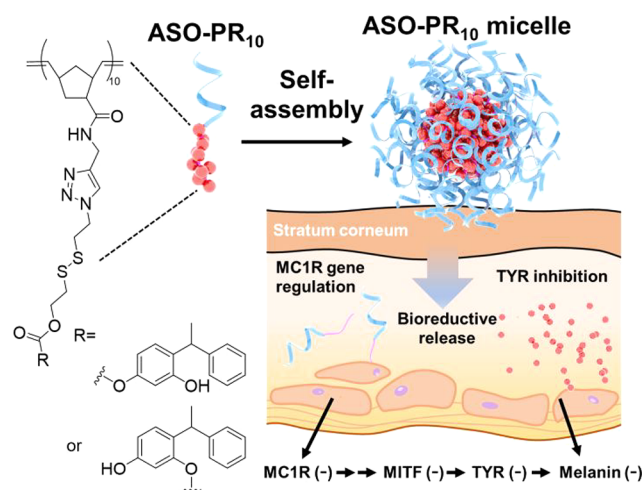
Here, we report an SNA-based skin depigmentation agent incorporating an antisense oligonucleotide (ASO) targeting MC1R (to downregulate new TYR synthesis) and a polymerized PR prodrug, which releases active PR bio-reductively upon cell internalization (to disable existing TYR). The SNA takes advantage of the amphiphilicity of the ASO–drug conjugate,^{22,23} allowing for the formation of a spherical micelle with a dense DNA shell that is structurally analogous to prototypical SNAs (Scheme 1). The ASO component functions as both a carrier and a payload, enhancing drug water solubility and transdermal delivery of both components while being an active agent for gene regulation. It has been shown that the antisense SNAs regulate gene expression by RNase H-mediated degradation of target mRNA without the ASO being released.²⁴

The amphiphile is assembled by copper-free click chemistry using an ASO modified with a 5'-dibenzocyclooctyne (DBCO) and an azide-functionalized prodrug polymer (Scheme S1). Because of the lack of an established MC1R ASO sequence, we screened a number of sequences against the MC1R mRNA in murine melanoma B16F10 cells using lipofectamine 2k-formulated ASOs and identified a sequence with reasonable antisense activity (sequence: 5'-TTCTCCACCA-GACTCACCA-3', Figure S1).^{25–27} The polymer is synthesized via sequential ring-opening metathesis polymerization of two monomers, an oxanorbornene bromide (N-Br)²⁸ and a norbornene disulfide PR (N-SS-PR),²³ which gives a narrowly

Received: November 17, 2020

Published: January 12, 2021



Scheme 1. Structure of ASO-PR₁₀ Prodrug Conjugate and Their Micellar SNA Assembly^a

^aUpon skin penetration, bioactive PR and ASO are released.

dispersed diblock copolymer (PDI = 1.2, M_w = 7.0 kDa, Figure S2) with high yield (~98%). Azide substitution of the bromide is carried out postpolymerization. A bioreductive, self-immolative disulfide linker is incorporated in N-SS-PR,²⁹ which can be cleaved under intracellular reductive conditions and release the active form of the drug. The ratio between PR and DNA is designed to be 10:1 (mol:mol) by controlling the stoichiometries during polymerization and final coupling. This ratio is balanced to provide sufficient driving force for micellization while also maintaining solubility during polymerization and coupling. The coupling reaction is performed in a dimethylformamide (DMF)/water (5:1, v/v) mixture, giving a yield of ~68% based on gel electrophoresis band densitometry analysis (Figure 1A).

The ASO-PR₁₀ amphiphile readily forms spherical micellar nanoparticles in an aqueous buffer. Dynamic light scattering

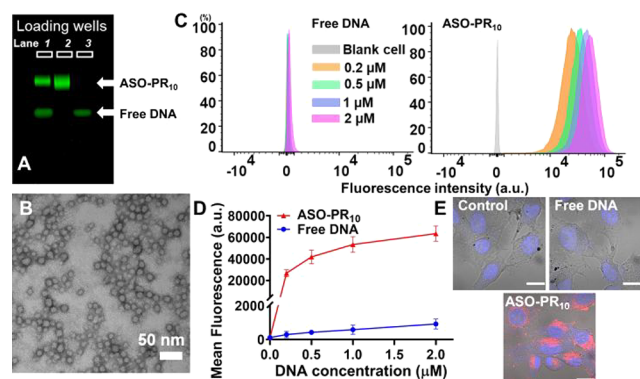


Figure 1. (A) Agarose gel (2%) electrophoresis of the conjugation reaction mixture (lane 1) between N₃-PR₁₀ and DBCO-ASO, purified ASO-PR₁₀ conjugate (lane 2), and free ASO (lane 3). (B) TEM image of the ASO-PR₁₀ nanoparticles. Samples were stained with uranyl acetate (2%). (C, D) Flow cytometry measurement of B16F10 cells treated with Cy5-labeled ASO-PR₁₀ SNAs or Cy5-labeled free ASO (0.2–2 μM ASO, 4 h), showing significantly (>100×) higher uptake for the SNAs. Error bar: mean ± SD; n = 3. (E) Confocal microscopy imaging of cells treated with 2 μM of Cy5-labeled ASO-PR₁₀ nanoparticles or free ASO. Images taken with identical settings. Scale bar: 20 μm.

shows the presence of nanoparticles with a number-average hydrodynamic diameter of 18.4 ± 5.2 nm (Figure S3, Table S2) and a zeta potential of -21.8 ± 4.8 mV. The formation of micelles is also confirmed by transmission electron microscopy (TEM), which shows spherical particles with dry-state sizes averaging 15.2 ± 1.4 nm (Figure 1B). To test if the PR component can be released, dithiothreitol (DTT) is used to simulate the reductive intracellular environment. When treated with 10 mM DTT at 37 °C for 1–4 h, a faster-migrating band emerged during gel electrophoresis, which is likely the monomeric form of the PR-free DNA–polymer conjugate (Figure S4). The released compound matches unmodified PR in mass (measured by electrospray ionization mass spectrometry) and in retention time during reverse-phase HPLC analysis (Figure S5).

To examine the cellular uptake of the ASO-PR₁₀ nanoparticles, B16F10 cells were treated with Cy5-labeled nanoparticles or free DNA in the concentration range of 0.2 to 2 μM (DNA basis). ASO-PR₁₀-treated cells exhibit ~100 times higher cellular uptake than free ASO-treated cells, as evidenced by flow cytometry (Figure 1C,D). The high level of uptake is corroborated by confocal laser scanning microscopy, which shows strong fluorescence signals in the cytoplasm of the cells treated with ASO-PR₁₀ nanoparticles but only background signals for ASO- and vehicle (phosphate-buffered saline, PBS)-treated cells (Figure 1E). The high cell uptake of SNA-type nanoparticles has been shown to be the result of class A scavenger receptors-mediated endocytosis via a lipid-raft-dependent, caveolae-mediated pathway (Figure S6).³⁰ Pretreatment of B16F10 cells with the pharmacological inhibitor methyl-β-cyclodextrin (which depletes and removes cholesterol) significantly reduces intracellular accumulation of Cy5-labeled ASO-PR₁₀, which is consistent with prior mechanistic studies. Despite high cellular uptake, the ASO-PR₁₀ particles exhibit negligible levels of cytotoxicity in the concentration range tested, 1–20 μM (PR basis), by a 3-(4,5-dimethylthiazol-2-yl)-2,5-diphenyltetrazolium bromide cytotoxicity assay (Figure S7). In addition, the cells are morphologically identical to untreated cells by microscopic evaluation.

Next, we compare the antimelanogenic efficacy of ASO-PR₁₀ nanoparticles, free PR, DNA-PR₁₀ nanoparticle with a scrambled sequence (Scr-PR₁₀), and PR-devoid ASO micelles *in vitro* by measuring tyrosinase inhibition and melanin content. B16F10 cells were treated with α-MSH (200 nM) to stimulate melanin formation. When ASO-PR₁₀ nanoparticles and equivalent amounts of free PR (2 to 20 μM PR) were added, the effects of α-MSH were reversed in a dose-dependent manner. Remarkably, the ASO-PR₁₀ particles show comparable reduction in tyrosinase activity to molecular PR despite that the latter is able to freely diffuse into the cell (inferred from an octanol/water partition coefficient value of 3.35),³¹ while the particles require bioreductive activation (Figure 2A). Furthermore, a potent antimelanogenic effect is observed for both ASO-PR₁₀ and PR as determined by measuring the intracellular melanin content using light absorbance at 405 nm, corroborating the efficient intracellular release of PR in the active form by the micelles (Figures 2B, S8). To measure the antisense activity of the ASO-PR₁₀ SNAs, MC1R levels from B16F10 cell lysates were measured by Western blot. SNAs reduced MC1R levels in a dosage-dependent manner, with a maximum reduction level (83%) achieved at 2 μM ASO (20 μM PR). The effect is not a feedback loop of released molecular PR, as PR itself does not

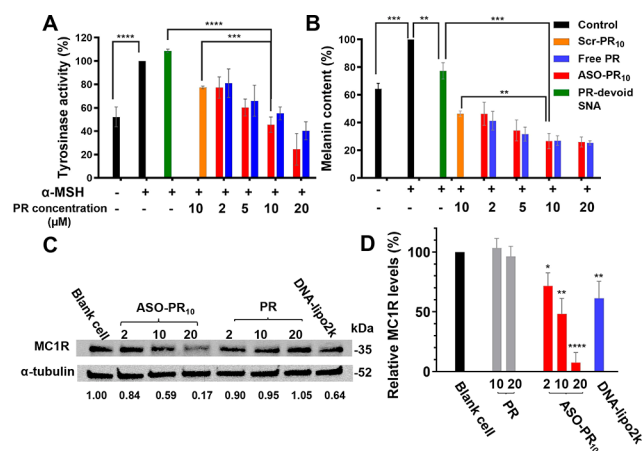


Figure 2. Tyrosinase activity (A) and melanin content (B) upon treatment with ASO-PR₁₀, DNA-PR₁₀ with a scrambled sequence (Scr-PR₁₀), PR-devoid micelles (in PBS), or free PR (in DMSO). α -MSH is used to stimulate melanogenesis. Tyrosinase activity and melanin content are recorded as percent changes compared with α -MSH-treated cells (2 to 20 μ M PR, 48 h treatment). PR-devoid micelles: 1 μ M ASO. (C, D) MC1R levels in B16F10 cells after treatment with PR, ASO-PR₁₀, and controls (2 to 20 μ M PR, 72 h treatment) as determined by Western blot analysis. DNA-lipo2k complexes: 10 μ M ASO. * p < 0.05, ** p < 0.01, *** p < 0.001, **** p < 0.0001 (two-tailed test).

cause changes in MC1R levels at the same PR concentration (Figure 2C,D). Interestingly, ASO-PR₁₀ particles show slightly better reduction in tyrosinase activity and melanin content than both Scr-PR₁₀ and PR-devoid particles, suggesting some level of synergy between the ASO and PR. Collectively, these results show that the drug and ASO components in the ASO-PR₁₀ serve as an effective delivery vehicle for each other through the formation of SNAs but retain their bioactivity upon cellular uptake.

In order to examine the degrees of skin penetration and depigmentation, C57BL/6 mice are used as a model. Because the epidermis of the mice ear skin contains epidermal melanocytes, unlike the trunk/fur-bearing skin, the ear skin region is selected for testing.^{32,33} Cy5-labeled ASO-PR₁₀ SNAs, Cy5-labeled free ASO, and free Cy5 dye (equivalent to 10 μ M DNA, dispersed in Nanopure water) were topically applied to hairless ear skin every 8 h for a total of four times. Fluorescence microscopy of sectioned ear skin revealed significant fluorescence in the matrix of the stratum corneum, the cytoplasm of epidermal cells, and the dermis for the ASO-PR₁₀-treated sample but not for control-treated samples (Figures 3A, S9). To test the efficacy of the SNA in suppressing melanogenesis, the SNA, PR, or vehicle was topically applied daily for 32 days to the dorsal ear skin of the mouse. To minimize differences among individuals, the right ear of each mouse receives SNA or PR while the left ear is treated with an equal volume of vehicle. Due to the poor solubility of PR in water, a mixed solvent of 1,2-propanediol/ethanol (v/v 3:7) was used as vehicle, while the SNAs remain dispersed in water. On days 8 through 22, mice were exposed to 200 mJ/cm² of UVB irradiation every other day to induce hyperpigmentation (Figure S10). The degree of depigmentation is quantitatively evaluated by comparing the skin color between the two ears of mice. The skin lightness was measured in reflectance by colorimetry using a tristimulus colorimeter and shown as L^* , which is the lightness component in the

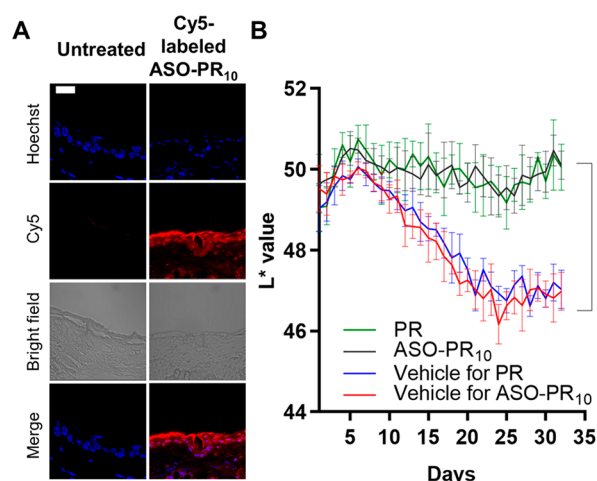


Figure 3. (A) Fluorescence micrographs of mouse ear sections (paraffin-embedded) after treatment with Cy5-labeled ASO-PR₁₀ (red). Cell nuclei are stained with Hoechst 33342 (blue). ASO-PR₁₀ fluorescence is present throughout the stratum corneum, epidermis, and dermis. Scale bar: 20 μ m. (B) Brightness levels (L^* value) in mouse left (blue/red) and right (green/black) ears upon treatment with sample/vehicle groups for 32 days. **** p < 0.0001 (two-tailed test).

CIELAB color space. The darkest black is represented by L^* = 0, and the brightest white at L^* = 100. The L^* values of both ears of mice were recorded daily (Figure 3B). During days 8 to 22, UVB irradiation induced significant melanogenesis in both vehicle-treated groups as reflected in a decrease of L^* values, with an average ΔL^* of -2.9 ± 0.5 (water) and -2.8 ± 0.6 (1,2-propanediol/ethanol). Strikingly, the ASO-PR₁₀- and PR-treated groups both exhibited insignificant changes in L^* , suggesting successful blockage of melanogenesis. Upon termination of UVB irradiation, the vehicle-treated groups cease to further darken, while the ASO-PR₁₀- and PR-treated groups lighten slightly, with ΔL^* being $\sim +0.5 \pm 0.7$ and $+0.4 \pm 0.3$, respectively. Overall, comparing day 32 to day 1, both PR and SNA produced a net skin lightening effect despite UVB irradiation for 2 weeks, while both control groups exhibited a visible darkening effect (Figure S11). Collectively, these results support that the PR-loaded SNA can deliver the active ingredients through the stratum corneum to induce a protective, antimelanogenic effect and avoid hyperpigmentation upon topical application.

To further study the effect of ASO-PR₁₀ on a tissue level, the distribution of melanin at the epidermis layer was visualized by Fontana–Masson staining. There is clearly a higher level of melanin in the epidermis of the vehicle-treated left ear, as demonstrated by deposits of melanin (indicated by the arrows), whereas treatment by PR or ASO-PR₁₀ decreased melanin content in the epidermis to levels comparable to nontreated control (Figure 4A). To test the antisense efficacy of the SNA in suppressing MC1R expression, MC1R protein was detected by immunohistochemistry (IHC) staining (Figure S12). While both vehicle- and SNA-treated tissues exhibit fluorescence associated with MC1R, the intensity for the ASO-PR₁₀ is $\sim 50\%$ that of the vehicle-treated control (Figure 4B). However, the reduction may not have contributed to the overall phenotypic response, as the SNA does not show an advantage in activity despite having the ability to reduce MC1R levels. This observation may be due to insufficient treatment time, incomplete depletion of target protein,¹⁵ or the

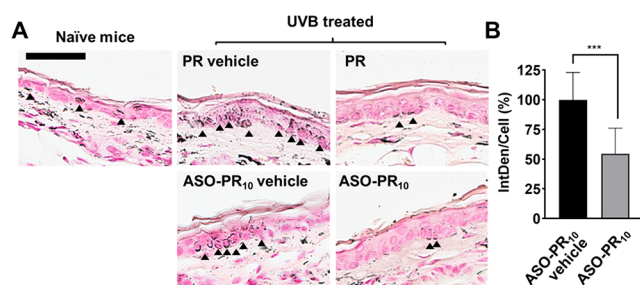


Figure 4. (A) Histological analysis of sectioned mouse ear after treatment with PR/ASO-PR₁₀/vehicle groups (paraffin-embedded). Melanin (indicated by black arrows) is stained by Fontana–Masson staining. Scale bar: 50 μm . (B) Relative MC1R levels in ASO-PR₁₀- vs vehicle-treated mouse ears as determined by immunohistostaining. *** $p < 0.001$ (two-tailed test).

fact that PR by itself can effectively suppress TYR activity once delivered to the cell. However, the poor water solubility of PR requires a harsh solvent condition to be used, which may cause skin drying and irritations. For better synergy, future designs may target alternative pathways such as MC1R-free tyrosinase biosynthesis initiated by p53.³⁴

In summary, we have synthesized an SNA-like micellar nanoparticle with a tyrosinase inhibitor prodrug core and an ASO shell that can inhibit the expression of a key receptor involved in melanogenesis. This drug-cored SNA can penetrate the ear skin of mice upon direct topical application. Once inside the melanocytes, the drug component is released via cleavage of a bioreductive, self-immolative linker, while the ASO inhibits target gene expression. This approach takes advantage of otherwise weaknesses associated with highly hydrophobic drug molecules and non-cell-penetrating ASOs and transforms them into essential features that enable their co-delivery across the skin and into skin cells. The principles demonstrated here should be broadly applicable for drug/oligonucleotide combination therapies that target a variety of skin-related disorders via topical application.

■ ASSOCIATED CONTENT

Supporting Information

The Supporting Information is available free of charge at <https://pubs.acs.org/doi/10.1021/jacs.0c12044>.

Materials and methods, experimental procedures, instrumentation, supplemental figures, and references (PDF)

■ AUTHOR INFORMATION

Corresponding Author

Ke Zhang – Department of Chemistry and Chemical Biology, Northeastern University, Boston, Massachusetts 02115, United States; orcid.org/0000-0002-8142-6702; Email: k.zhang@northeastern.edu

Authors

Yang Fang – Department of Chemistry and Chemical Biology, Northeastern University, Boston, Massachusetts 02115, United States

Xueguang Lu – Department of Chemistry, Massachusetts Institute of Technology, Cambridge, Massachusetts 02139, United States

Dali Wang – Department of Chemistry and Chemical Biology, Northeastern University, Boston, Massachusetts 02115, United States

Jiansong Cai – Department of Chemistry and Chemical Biology, Northeastern University, Boston, Massachusetts 02115, United States

Yuyan Wang – Department of Chemistry and Chemical Biology, Northeastern University, Boston, Massachusetts 02115, United States

Peiru Chen – Department of Chemistry and Chemical Biology, Northeastern University, Boston, Massachusetts 02115, United States

Mengqi Ren – Department of Chemistry and Chemical Biology, Northeastern University, Boston, Massachusetts 02115, United States

Hao Lu – Department of Chemistry and Chemical Biology, Northeastern University, Boston, Massachusetts 02115, United States

Jennifer Union – Department of Chemistry and Chemical Biology, Northeastern University, Boston, Massachusetts 02115, United States

Lei Zhang – Department of Chemistry and Chemical Biology, Northeastern University, Boston, Massachusetts 02115, United States

Yehui Sun – Department of Chemistry and Chemical Biology, Northeastern University, Boston, Massachusetts 02115, United States

Fei Jia – Department of Chemistry and Chemical Biology, Northeastern University, Boston, Massachusetts 02115, United States

Xi Kang – Department of Chemistry and Chemical Biology, Northeastern University, Boston, Massachusetts 02115, United States

Xuyu Tan – Department of Chemistry and Chemical Biology, Northeastern University, Boston, Massachusetts 02115, United States; Department of Chemistry, Massachusetts Institute of Technology, Cambridge, Massachusetts 02139, United States

Complete contact information is available at: <https://pubs.acs.org/10.1021/jacs.0c12044>

Author Contributions

K.Z., Y.F., and X.T. devised the experiments and wrote the manuscript. Y.F. conducted the synthesis of materials, purification, and material/biological characterization. All other authors contributed to material synthesis, purification, and/or discussion of the results. All authors edited the manuscript.

Notes

The authors declare no competing financial interest.

■ ACKNOWLEDGMENTS

This publication was made possible by the National Science Foundation (DMR award number 2004947) and the National Institute of General Medical Sciences (award number 1R01GM121612). The authors thank Dr. Heather Clark for assistance with confocal microscopy, Dr. William Fowle for electron microscopy, Dr. Jiahe Li for flow cytometry, and Dr. Roman Manetsch for mass spectrometry.

REFERENCES

- (1) Rigopoulos, D.; Gregoriou, S.; Katsambas, A. Hyperpigmentation and melasma. *J. Cosmet. Dermatol.* **2007**, *6*, (3) 195–202.
- (2) D’Mello, S. A. N.; Finlay, G. J.; Baguley, B. C.; Askarian-Amiri, M. E. Signaling Pathways in Melanogenesis. *Int. J. Mol. Sci.* **2016**, *17*, 1144.
- (3) Kim, Y. J.; Uyama, H. Tyrosinase inhibitors from natural and synthetic sources: structure, inhibition mechanism and perspective for the future. *Cell. Mol. Life Sci.* **2005**, *62* (15), 1707–23.
- (4) del Marmol, V.; Beermann, F. Tyrosinase and related proteins in mammalian pigmentation. *FEBS Lett.* **1996**, *381* (3), 165–168.
- (5) Chao, H.-C.; Najjaa, H.; Villareal, M. O.; Ksouri, R.; Han, J.; Neffati, M.; Isoda, H. Arthropodium scoparium inhibits melanogenesis through the down-regulation of tyrosinase and melanogenic gene expressions in B16 melanoma cells. *Exp. Dermatol.* **2013**, *22* (2), 131–136.
- (6) Chiang, H.-M.; Chien, Y.-C.; Wu, C.-H.; Kuo, Y.-H.; Wu, W.-C.; Pan, Y.-Y.; Su, Y.-H.; Wen, K.-C. Hydroalcoholic extract of *Rhodiola rosea* L. (Crassulaceae) and its hydrolysate inhibit melanogenesis in B16F0 cells by regulating the CREB/MITF/tyrosinase pathway. *Food Chem. Toxicol.* **2014**, *65*, 129–139.
- (7) Suzuki, I.; Cone, R. D.; Im, S.; Nordlund, J.; Abdel-Malek, Z. A. Binding of melanotropic hormones to the melanocortin receptor MC1R on human melanocytes stimulates proliferation and melanogenesis. *Endocrinology* **1996**, *137* (5), 1627–1633.
- (8) Valverde, P.; Healy, E.; Jackson, I.; Rees, J. L.; Thody, A. J. Variants of the melanocyte-stimulating hormone receptor gene are associated with red hair and fair skin in humans. *Nat. Genet.* **1995**, *11* (3), 328–330.
- (9) Nouri, K.; Bowes, L.; Chartier, T.; Romagosa, R.; Spencer, J. Combination Treatment of Melasma with Pulsed CO₂ Laser Followed by Q-Switched Alexandrite Laser: A Pilot Study. *Dermatol. Surg.* **1999**, *25* (6), 494–497.
- (10) Draeos, Z. D. Skin lightening preparations and the hydroquinone controversy. *Dermatol Ther.* **2007**, *20* (5), 308–313.
- (11) Lim, J. T. E. Frcpi; Fams, Treatment of Melasma Using Kojic Acid in a Gel Containing Hydroquinone and Glycolic Acid. *Dermatol. Surg.* **1999**, *25* (4), 282–284.
- (12) Fan, H.; Liu, G.; Huang, Y.; Li, Y.; Xia, Q. Development of a nanostructured lipid carrier formulation for increasing photo-stability and water solubility of Phenylethyl Resorcinol. *Appl. Surf. Sci.* **2014**, *288*, 193–200.
- (13) Chang, T. S. An updated review of tyrosinase inhibitors. *Int. J. Mol. Sci.* **2009**, *10* (6), 2440–75.
- (14) Kim, B.-S.; Na, Y.-G.; Choi, J.-H.; Kim, I.; Lee, E.; Kim, S.-Y.; Lee, J.-Y.; Cho, C.-W. The Improvement of Skin Whitening of Phenylethyl Resorcinol by Nanostructured Lipid Carriers. *Nanomaterials* **2017**, *7*, 241.
- (15) Yi, X.; Zhao, G.; Zhang, H.; Guan, D.; Meng, R.; Zhang, Y.; Yang, Q.; Jia, H.; Dou, K.; Liu, C.; Que, F.; Yin, J. Q. MITF-siRNA Formulation Is a Safe and Effective Therapy for Human Melasma. *Mol. Ther.* **2011**, *19* (2), 362–371.
- (16) Chen, M.; Zakrewsky, M.; Gupta, V.; Anselmo, A. C.; Slee, D. H.; Muraski, J. A.; Mitragotri, S. Topical delivery of siRNA into skin using SPACE-peptide carriers. *J. Controlled Release* **2014**, *179*, 33–41.
- (17) Barua, S.; Mitragotri, S. Challenges associated with penetration of nanoparticles across cell and tissue barriers: A review of current status and future prospects. *Nano Today* **2014**, *9* (2), 223–243.
- (18) Carter, P.; Narasimhan, B.; Wang, Q. Biocompatible nanoparticles and vesicular systems in transdermal drug delivery for various skin diseases. *Int. J. Pharm.* **2019**, *555*, 49–62.
- (19) Lopez, R. F. V.; Seto, J. E.; Blankschtein, D.; Langer, R. Enhancing the transdermal delivery of rigid nanoparticles using the simultaneous application of ultrasound and sodium lauryl sulfate. *Biomaterials* **2011**, *32* (3), 933–941.
- (20) Zheng, D.; Giljohann, D. A.; Chen, D. L.; Massich, M. D.; Wang, X.-Q.; Iordanov, H.; Mirkin, C. A.; Paller, A. S. Topical delivery of siRNA-based spherical nucleic acid nanoparticle conjugates for gene regulation. *Proc. Natl. Acad. Sci. U. S. A.* **2012**, *109* (30), 11975.
- (21) Liu, H.; Kang, R. S.; Bagnowski, K.; Yu, J. M.; Radecki, S.; Daniel, W. L.; Anderson, B. R.; Nallagatla, S.; Schook, A.; Agarwal, R.; Giljohann, D. A.; Paller, A. S. Targeting the IL-17 Receptor Using Liposomal Spherical Nucleic Acids as Topical Therapy for Psoriasis. *J. Invest. Dermatol.* **2020**, *140* (2), 435–444.
- (22) Tan, X.; Li, B. B.; Lu, X.; Jia, F.; Santori, C.; Menon, P.; Li, H.; Zhang, B.; Zhao, J. J.; Zhang, K. Light-Triggered, Self-Immolative Nucleic Acid-Drug Nanostructures. *J. Am. Chem. Soc.* **2015**, *137* (19), 6112–6115.
- (23) Tan, X.; Lu, X.; Jia, F.; Liu, X.; Sun, Y.; Logan, J. K.; Zhang, K. Blurring the Role of Oligonucleotides: Spherical Nucleic Acids as a Drug Delivery Vehicle. *J. Am. Chem. Soc.* **2016**, *138* (34), 10834–10837.
- (24) Prigodich, A. E.; Alhasan, A. H.; Mirkin, C. A. Selective Enhancement of Nucleases by Polyvalent DNA-Functionalized Gold Nanoparticles. *J. Am. Chem. Soc.* **2011**, *133* (7), 2120–2123.
- (25) Li, D.; Taylor, A. W. Diminishment of alpha-MSH anti-inflammatory activity in MC1r siRNA-transfected RAW264.7 macrophages. *J. Leukocyte Biol.* **2008**, *84* (1), 191–8.
- (26) Seong, I.; Min, H. J.; Lee, J. H.; Yeo, C. Y.; Kang, D. M.; Oh, E. S.; Hwang, E. S.; Kim, J. Sox10 controls migration of B16F10 melanoma cells through multiple regulatory target genes. *PLoS One* **2012**, *7* (2), No. e31477.
- (27) Chung, H.; Lee, J. H.; Jeong, D.; Han, I. O.; Oh, E. S. Melanocortin 1 receptor regulates melanoma cell migration by controlling syndecan-2 expression. *J. Biol. Chem.* **2012**, *287* (23), 19326–35.
- (28) Lu, X.; Jia, F.; Tan, X.; Wang, D.; Cao, X.; Zheng, J.; Zhang, K. Effective Antisense Gene Regulation via Noncationic, Polyethylene Glycol Brushes. *J. Am. Chem. Soc.* **2016**, *138* (29), 9097–9100.
- (29) Deng, Z.; Hu, J.; Liu, S. Disulfide-Based Self-Immolative Linkers and Functional Bioconjugates for Biological Applications. *Macromol. Rapid Commun.* **2020**, *41* (1), 1900531.
- (30) Choi, C. H. J.; Hao, L.; Narayan, S. P.; Auyeung, E.; Mirkin, C. A. Mechanism for the endocytosis of spherical nucleic acid nanoparticle conjugates. *Proc. Natl. Acad. Sci. U. S. A.* **2013**, *110* (19), 7625.
- (31) Zhang, Y.; Sil, B. C.; Kung, C. P.; Hadgraft, J.; Heinrich, M.; Sinko, B.; Lane, M. E. Characterization and topical delivery of phenylethyl resorcinol. *Int. J. Cosmet. Sci.* **2019**, *41* (5), 479–488.
- (32) Nordlund, J. J.; Collins, C. E.; Rheins, L. A. Prostaglandin E2 and D2 but Not MSH Stimulate the Proliferation of Pigment Cells in the Pinnal Epidermis of the DBA/2 Mouse. *J. Invest. Dermatol.* **1986**, *86* (4), 433–437.
- (33) Kumar, K. J.; Vani, M. G.; Wang, S. Y.; Liao, J. W.; Hsu, L. S.; Yang, H. L.; Hseu, Y. C. In vitro and in vivo studies disclosed the depigmenting effects of gallic acid: a novel skin lightening agent for hyperpigmentary skin diseases. *Bio Factors (Oxford, England)* **2013**, *39* (3), 259–70.
- (34) Schallreuter, K. U.; Kothari, S.; Chavan, B.; Spencer, J. D. Regulation of melanogenesis - controversies and new concepts. *Exp. Dermatol.* **2008**, *17* (5), 395–404.